Supplementary Materials for

Gene-Microbiota Interactions Contribute to the Pathogenesis of Inflammatory Bowel Disease

Hiutung Chu[1*], Arya Khosravi[1], Indah P. Kusumawardhani[1], Alice H.K. Kwon[1], Anilton C. Vasconcelos[2], Larissa D. Cunha[3], Anne E. Mayer[4], Yue Shen[1], Wei-Li Wu[1], Amal Kambal[4], Stephan R. Targan[5], Ramnik J. Xavier[6], Peter B. Ernst[2], Douglas R. Green[3], Dermot P.B. McGovern[5], Herbert W. Virgin[4], and Sarkis K. Mazmanian[1*]

[*]Correspondences to: hiuchu@caltech.edu and sarkis@caltech.edu

This PDF file includes:

Materials and Methods

Mice

C57BL/6 mice were purchased from Taconic Farms. *Nod2*$^{-/-}$ mice were purchased from the Jackson Laboratory. *Atg16l1*$^{fl/fl}$ *Cd11c*-Cre$^{-/-}$ (WT), *Atg16l1*$^{fl/fl}$ C*d11c*-Cre$^{+/-}$ (Atg16L1$^{\Delta CD11c}$), *Atg16l1*$^{fl/fl}$ *LysM*-Cre, *Atg5*$^{fl/fl}$ *LysM*-Cre, *Atg7*$^{fl/fl}$ *LysM*-Cre, *Atg14*$^{fl/fl}$ *LysM*-Cre, *Fip200*$^{fl/fl}$ *LysM*-Cre mice and femurs were obtained from H. W. Virgin (*41, 42*), *ATG16L1* T300A mice from R. J. Xavier (*22*), and *Ulk1*$^{-/-}$ and *Rubicon*$^{-/-}$ mice and femurs from M. Kundu (*43*) and D. R. Green (*35*) under a materials transfer agreement with St. Jude Children's Research Hospital, respectively. For all studies performed with Cre-floxed mice, the Cre$^{-/-}$ littermates served as wildtype controls. 8-10 week old sex-matched mice were used in the study. All procedures were performed in accordance with the guidelines and approved protocols from the Institutional Animal Care and Use Committee at the California Institute of Technology.

Human peripheral blood mononulear cells

Crohn's disease subjects were recruited from the IBD Center at Cedars-Sinai Medical Center following informed consent and IRB approval. *ATG16L1* genotyping was performed using the Immunochip (Illumina, San Diego, CA, USA) according to the manufacturer's instructions and as previously described (*10*). Patient sample information is described in Supplemental Table 1.

Bacterial strains, culture conditions and OMV purification

Bacteroides fragilis strain NCTC9343, *Bacteroides thetaiotamicron* ATCC 29148 and

Bacteroides vulgatus ATCC 8482 were obtained from the American Type Culture Collection, and *B. fragilis*ΔPSA has been described previously (*44*). *Bacteroides* strains were grown anaerobically (80% N_2, 10% H_2, 10% CO_2) at 37ºC in brain heart infusion broth (BD Biosciences) supplemented with 5 μg/ml hemin (Sigma) and 0.5 μg/ml vitamin K (Sigma). *Salmonella enterica* serovar Typhimurium (IR715), a nalidixic acid-resistant strain of 14028, was a generous gift from A. Bäumler. *S.* Typhimurium were grown aerobically at 37°C in Luria-Bertani (LB) broth. For the induction of OMVs*,* *Bacteroides* strains were grown in minimal media, which consisted of RPMI 1640, no phenol red (Life Technologies) supplemented with 1% fetal bovine serum (Life Technologies), 8 mg/ml glucose (Sigma), 2.5 μg/ml hemin (Sigma) and 0.25 μg/ml vitamin K (Sigma). *B. fragilis* OMV isolation was performed as previously described (*32*). Briefly, electron dense layer-enriched *B. fragilis* (*45*) was grown in minimal media for 24 hr anaerobically. OMVs were recovered from the bacteria-free culture supernatant by ultracentrifugation, washed, resuspended in PBS and filtered through a 0.4 μm filter (Millipore) prior to treatment of cell cultures or oral gavage of mice.

Experimental colitis

WT (*Atg16l1*$^{fl/fl}$ *Cd11c*-Cre$^{-/-}$), ATG16L1-deficient (*Atg16l1*$^{fl/fl}$ C*d11c*-Cre$^{+/-}$; Atg16L1$^{\Delta CD11c}$), *ATG16L1* T300A, or *Nod2*$^{-/-}$ mice were orally gavaged with PBS or WT-OMV (5 μg) every other day for one week prior to 2,4-dinitrobenzenesulfonic acid (DNBS; Sigma) administration. On day 7, mice were anesthetized with isofluorane, and rectal administration of 5% DNBS in 50% ethanol was applied through a 3.5F catheter (Instech Solomon), as previously described (*32*). Control groups received ethanol

(Sham). Briefly, a flexible silicone catheter was inserted 4 cm into the colon, and the mice were held in a vertical position for at least 1 min after rectal administration. Mice were monitored and weighed daily for the duration of the experiment. Upon sacrifice, gut tissue was harvested, fixed in neutral 10% buffered formalin, embedded in paraffin, sectioned and stained with hematoxylin and eosin (H&E). All histology was evaluated in a blinded analysis by two veterinarians using a comprehensive scoring system. Hematoxylin-eosin-stained slides were scanned and digitally scored using a while slide imaging system (Hamamatsu NanoZoomer Slide Scanner 2.0HT). Slides were read using software (Hamamatsu NanoZoomer Viewer NDP.View 2.3.1) to allow the use of a web-based file-sharing platform. Colitis was classified into acute, chronic and chronic active, depending on the existence of vascular reaction (hyperemia, edema, hemorrhage). In addition, the predominant types of leukocytes in the infiltrates were considered (polymorphonuclear and/or mononuclear). The extension and the nature of the lesions allowed defining the distribution (focal, multifocal, locally extensive or diffuse) and the intensity (discrete, moderate, severe, transmural). Scoring was based on a modification of an approach described previously (*46*). Briefly, the number and distribution of mucosal polymorphonuclear cells as well as mononuclear cells and epithelial cell damage were scored from 0 – 4. The submucosa was scored for cellular infiltrates from 0 – 3 while the thickening and cellular infiltrates in the muscularis were scored from 0 – 2. All photomicrographs were captured using NanoZoomer Viewer NDP View 2.3.1 and scored using the same criteria by two people (P.B.E. and A.C.V.), including a comparative pathologist (A.C.V).

In vitro DC-T cell co-culture

Co-culture of bone marrow-derived dendritic cells (BMDCs) and $CD4^+$ T cells were performed as previously described (*30, 32, 36*). Briefly, BMDCs were generated from bone marrow progenitor cells isolated from femurs of WT or $Atg16L1^{\Delta CD11c}$ mice in the presence of 20 ng/ml GM-CSF (Miltenyi) in complete RPMI media 1640 (10% fetal bovine serum, 50 U/ml penicillin, 50 µg/ml streptomycin, 2mM L-glutamine, 1mM sodium pyruvate, 1mM HEPES, and non-essential amino acids, and β-mercaptoethanol). BMDCs were pulsed with PBS, WT-OMVs (10 µg/ml), ΔPSA-OMVs (10 µg/ml) or pure PSA (50 µg/ml) for 18 – 22 hrs; OMVs with a protein content of 10 µg contain 50 µg of PSA. BMDCs were washed, and co-cultured with splenic $CD4^+$ T cells at a ratio of 1:10 (DC:$CD4^+$ T cells) in the presence of 0.1µg/ml anti-mouse CD3 and 5 ng/ml of recombinant human TGF-β (Peprotech). After 3 – 5 days of co-culture, supernatants were collected for enzyme-linked immunosorbent assay (ELISA) analysis and cells stained with specific antibodies and a viability dye for analysis by flow cytometry.

To generate monocyte-derived dendritic cell (MoDCs), human PBMCs were isolated from fresh whole blood the same day of harvest using Ficoll-Hypaque (GE Healthcare) gradient (density = 1.070 g/ml), followed by monocyte enrichment using the Human Monocyte Isolation Kit II (Miltenyi). For differentiation into MoDCs, monocytes were incubated with recombinant human IL-4 and GM-CSF (Peprotech) every two days in complete RPMI 1640 (5% human AB serum, 50 U/ml penicillin, 50 µg/ml streptomycin, 2mM L-glutamine, 1mM sodium pyruvate, 1mM HEPES, non-essential amino acids, β-mercaptoethanol). MoDCs were pulsed with PBS, *B. fragilis* OMVs or PSA for 18 – 22

hrs, washed, and co-cultured with syngeneic $CD4^+$ T cells, isolated using the Human CD4 Isolation Kit II (Miltenyi), at a ratio of 1:10 (DC:$CD4^+$ T cells) in the presence of 1 mg/ml anti-human CD3 (eBiosciences) and 5 ng/ml of recombinant human TGF-β (Peprotech). After 6 days of co-culture, cells were restimulated with phorbol 12-myristate 13-acetate (PMA) (Sigma) and ionomycin (Calbiochem) in the presence of GolgiPlug (BD Biosciences) for 4.5 hr, and stained with specific antibodies and a viability dye for analysis by flow cytometry.

In vitro T cell suppression assay

$CD4^+CD25^+$ T_{reg} cells were purified from *in vitro* BMDC-T cell co-cultures using magnetic microbeads (Miltenyi). $CD4^+CD25^-$ responder effector T cells (T_{eff}) were isolated from mouse spleens, labeled with 2.5 μM CFSE for 10 min at 37ºC in the dark, washed, and incubated with T_{reg} cells at various T_{reg}:T_{eff} ratios in the presence of 1 μg/ml anti-mouse CD3 (eBiosciences). Irradiated CD4-depleted mouse splenocytes served as antigen-presenting cells. Cultures were incubated for 48 and 72 hrs, cells were stained with specific antibodies and a viability dye, and analyzed by flow cytometry. Dilution of CFSE signal is a measure of proliferation, and inhibition of proliferation a measure of T_{reg} activity.

Isolations of cells from tissues

Isolation of colon lamina propria (cLP) lymphocytes was performed, as previously described (*30, 32, 36*). Briefly, colons were cut open longitudinally, and luminal contents flushed with ice-cold PBS. Colons were cut into 1 cm pieces and incubated for 20 min in

10 mM dithiothreitol (Sigma) with gentle shaking, followed by two incubations at 20 min in 20 mM EDTA (Sigma). Supernatants were removed and remaining tissue was incubated in 1 mg/ml Collagenase D (Sigma), 0.25 U/ml Dispase (Roche), and 0.5 mg/ml DNase I (Worthington). Cells were filtered through a 70 μm cell strainer (BD Falcon) and separated by a 40%/80% (v/v) Percoll (GE Healthcare) density gradient. Cells were washed prior to staining for flow cytometry.

MLN and spleens were processed by grinding tissues through 100 μm cell strainer (BD Falcon) to generate single cell suspensions. Splenic cells were treated with RBC lysis buffer (Sigma) and washed prior to staining for flow cytometry.

Flow cytometry, intracellular cytokine staining, and ELISA

Cells were incubated in 5% mouse serum for 15 min and stained for 20 min at 4ºC with either LIVE/DEAD fixable green or far red dead stain kit (Life Technologies), with empirically titrated concentrations of the following antibodies: PerCP-Cy5.5-conjugated anti-mouse CD4 (clone: RM4-5), PerCP-Cy5.5-conjugated anti-human CD4 (clone: OKT4), and/or PE-Cy7-conjugated anti-mouse CD4 (clone: RM4-5). For intracellular staining, cells were fixed and permeabilized with the Foxp3/Transcription factor buffer kit (eBioscience). Intracellular staining was performed using the following antibodies: FITC-conjugated anti-mouse IFNγ (clone: XMG1.2), PE-conjugated anti-mouse IL-10 (clone: JES5-16E3), PE-conjugated anti-human Foxp3 (clone: PCH101), PerCP-Cy5.5 anti-mouse IL-17A (clone: eBio17B7), APC-conjugated anti-mouse Foxp3 (clone: FJK-16s), and/or APC-conjugated anti-human IL-10 (clone: JES3-9D7). All antibodies were

purchased from eBioscience. ROS detection was performed as previously described (*35*). Briefly, BMDCs were incubated with 1μM dihydroethidium (Life Technologies) for 30 min at 37ºC in the dark. Cells were washed and acquired immediately. Cell acquisition was performed on a BD FACS Calibur (BD Biosciences) or Miltenyi MACSQuant (Miltenyi), and data was analyzed using FlowJo software suite (TreeStar). For ELISAs, cell supernatant from *in vitro* DC-T cell co-culture were collected and mouse IL-10 and IL-17A were measured using commercially available kits (eBiosciences).

RNA isolation and quantitative real time RT-PCR

BMDCs were harvested, washed, and immediately lysed in RLT buffer for RNA isolation using the RNeasy Mini Kit, according to manufacturer's protocol (Qiagen). 1 μg of RNA was reverse transcribed using iScript cDNA Synthesis Kit, according to manufacturer's protocol (Bio-Rad) and diluted to 10 ng/μl based on the input concentration of total RNA.

Gene specific primers were designed using MacVector software and synthesized by Integrated DNA Technologies. Real-time PCR for the mammalian house keeping gene β-actin was used to ensure that input RNA was equal among all samples. Real-time PCR was performed on cDNA using the ABI PRISM 7900 HT (ThermoFisher).

Western blot

BMDCs were washed with PBS and lysed with 1X RIPA buffer (EMD Millipore) with protease inhibitor cocktail (Roche). Protein concentration was determined using BCA protein assay (Pierce). Samples were analyzed on 4 - 20% Tris-Glycine gels (Novex) and

proteins were transferred to Immobilon-P PVDF membrane (EMD Millipore). The membrane was blocked in 5% nonfat dry milk and probed for α-PSA (1:1000) or α-mouse β-actin (1:3000) (Cell Signaling) rabbit polyclonal antibodies with a horseradish peroxidase (HRP)-conjugated goat α-rabbit secondary antibody (1:5000) (KPL) and developed using LumiGLO chemiluminescent substrate (KPL). Chemiluminescent signal was detected with the Gel Doc™ XR+ System (Bio-Rad).

Statistical analyses

Student's t-test was used for pairwise comparisons. Survival curve was analyzed using the Grehan-Breslow-Wilcoxin test. One-way and two-way ANOVA with Post-hoc Tukey test were used for comparisons among one or two or more groups, respectively, using the GraphPad PRISM software.

Fig. S1

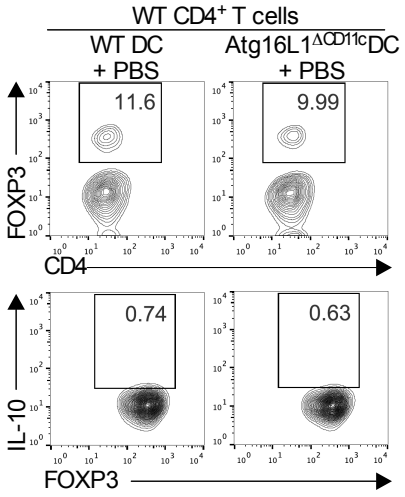

Fig. S1. Vehicle treatment of WT and Atg16L1$^{\Delta CD11c}$ DCs does not induce significant production of IL-10 among CD4$^+$Foxp3$^+$ T$_{regs}$.

Representative flow cytometry plots of CD4$^+$Foxp3$^+$IL-10$^+$ T$_{regs}$ from DC–T cell co-cultures with WT and Atg16L1$^{\Delta CD11c}$ DCs treated with PBS (vehicle). Data are representative of at least 3 independent experiments.

Fig. S2

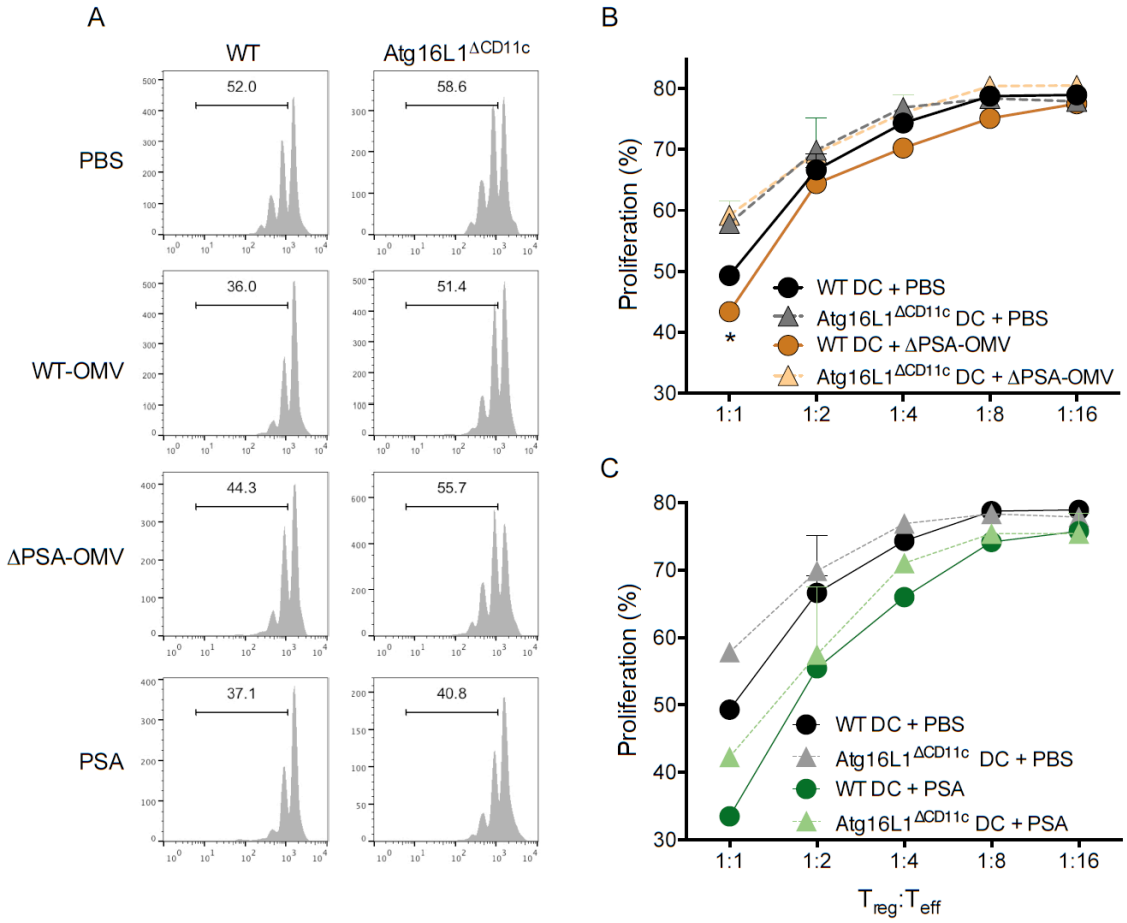

Fig. S2. Purified PSA does not require ATG16L1 to promote suppressive T_{reg} activity.

(A) Representative histrograms measuring suppression of responder T cell proliferation by *in vitro* generated T_{regs} from WT or Atg16L1$^{\Delta CD11c}$ DCs treated with PBS, *B. fragilis* WT-OMV, ΔPSA-OMV or purified PSA. **(B** and **C)** T cell suppression index of *in vitro* generated T_{regs} from WT or Atg16L1$^{\Delta CD11c}$ DCs treated with (B) ΔPSA-OMV or (C) purified PSA at various T_{reg}:T_{eff} ratios. Cell proliferation was stimulated with αCD3. Error bars represent S.E.M. *$p < 0.05$. Data are representative of at least 2 independent experiments.

Fig. S3

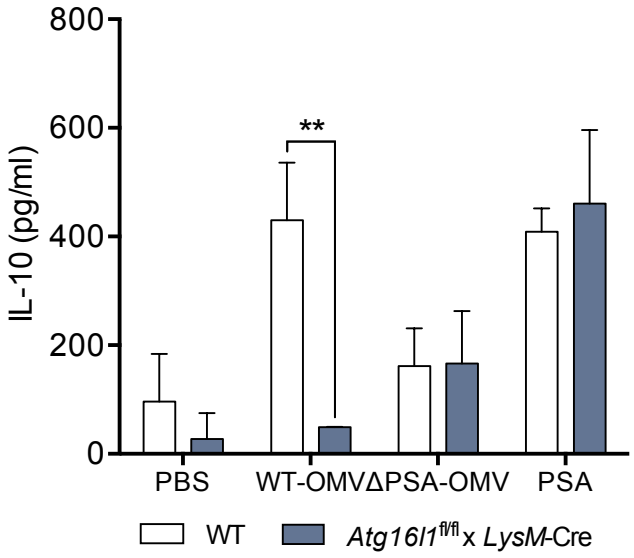

Fig. S3. *Atg16l1* $^{fl/fl}$ *LysMCre* DCs are unable to support *B. fragilis* OMV-induced IL-10 production.

ELISA for IL-10 production from DC–T cell co-cultures with WT or *Atg16l1*$^{fl/fl}$ *LysM*Cre DCs treated with PBS, *B. fragilis* WT-OMV, ΔPSA-OMV or purified PSA. Error bars represent S.E.M. ** $p < 0.01$. Data are representative of at least 2 independent experiments.

Fig. S4

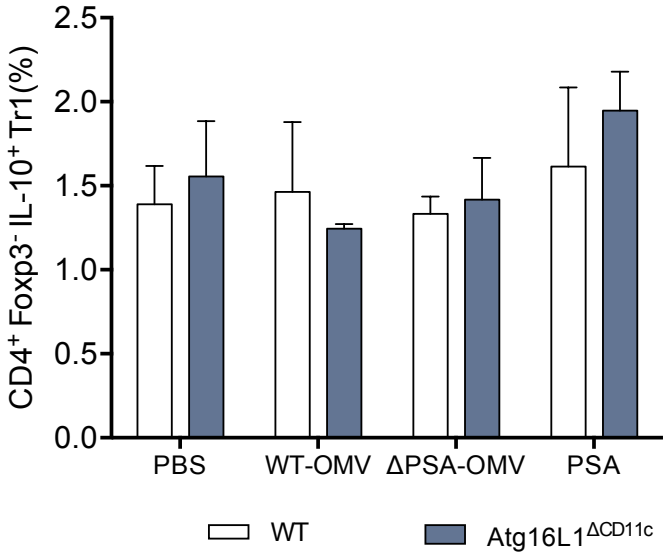

Fig. S4. *B. fragilis* OMVs do not induce IL-10 production among Foxp3$^-$ type 1 regulatory (Tr1) cells.

Frequency of CD4$^+$Foxp3$^-$IL-10$^+$ T_{regs} from DC–T cell co-cultures with WT or Atg16L1$^{\Delta CD11c}$ DCs treated with PBS, *B. fragilis* WT-OMV, ΔPSA-OMV or purified PSA. Data are representative of 3 independent experiments.

Fig. S5

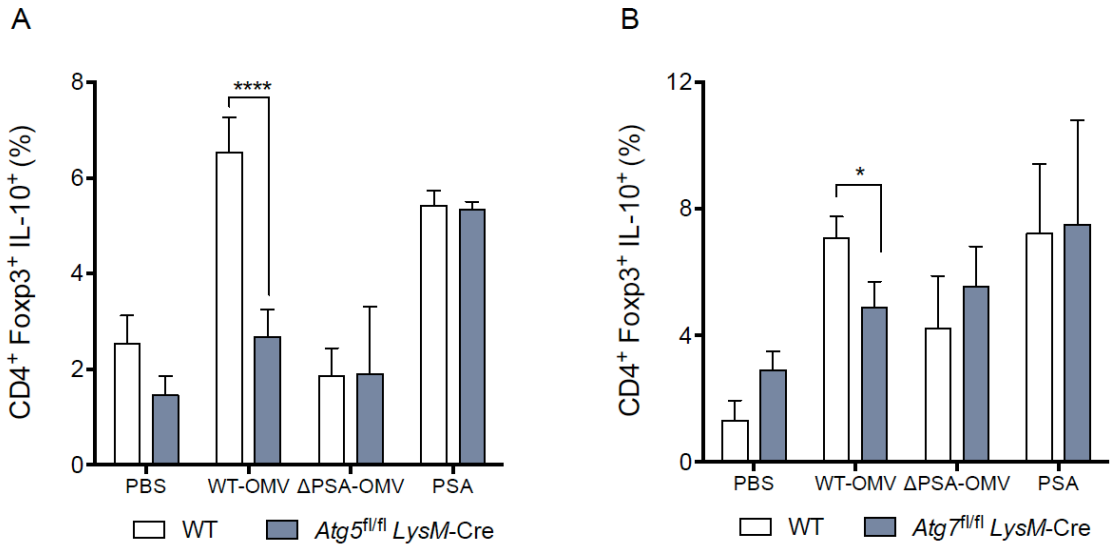

Fig. S5. *B. fragilis* OMVs require *Atg5* and *Atg7* to promote IL-10 production from Foxp3$^+$ T$_{regs}$.

Proportions of IL-10 expression among CD4$^+$ Foxp3$^+$ T$_{regs}$ following PBS, *B. fragilis* WT-OMV, ΔPSA-OMV or purified PSA treatment of **(A)** WT and *Atg5*$^{fl/fl}$ *LysM*Cre or **(B)** *Atg7*$^{fl/fl}$ *LysM*Cre BMDCs co-cultured with CD4$^+$ T cells. Error bars represent S.E.M. * $p < 0.05$, **** $p < 0.0001$. Data are representative of at least 3 independent experiments.

Fig. S6

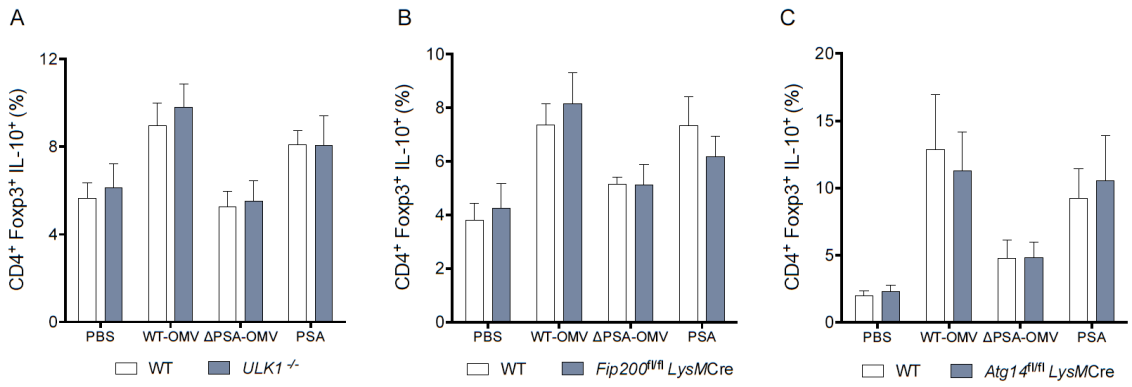

Fig. S6. *B. fragilis* OMVs do not require canonical autophagy to promote IL-10 production in Foxp3$^+$ T$_{regs}$.

The requirement of canonical autophagy was examined using **(A)** *Ulk*1$^{-/-}$, **(B)** *Fip200* $^{fl/fl}$ *LysM*Cre or **(C)** *Atg14* $^{fl/fl}$ *LysM*Cre BMDCs treated with PBS, *B. fragilis* WT-OMV, ΔPSA-OMV or purified PSA, then co-cultured with CD4$^+$ T cells. Measurement of IL-10$^+$ cells among the Foxp3$^+$ T$_{reg}$ population by flow cytometry. Error bars represent S.E.M. Data are representative of at least 3 independent experiments.

Fig. S7

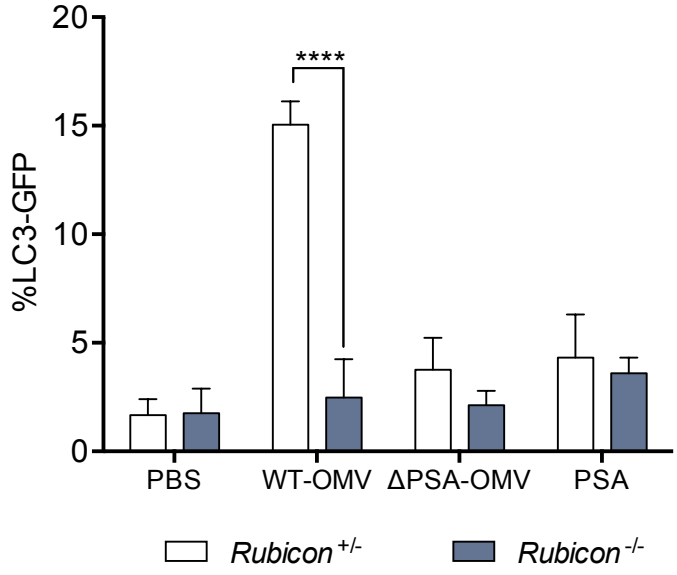

Fig. S7. *B. fragilis* WT-OMVs activate the LAP pathway.

Quantification of LC3-GFP accumulation upon 2h treatment of BMDCs with PBS, *B. fragilis* WT-OMV, ΔPSA-OMV or purified PSA in *Rubicon*$^{+/-}$ or *Rubicon*$^{-/-}$ DCs. Error bars represent S.E.M. **** $p < 0.0001$. Data are representative of 3 independent experiments.

Fig. S8

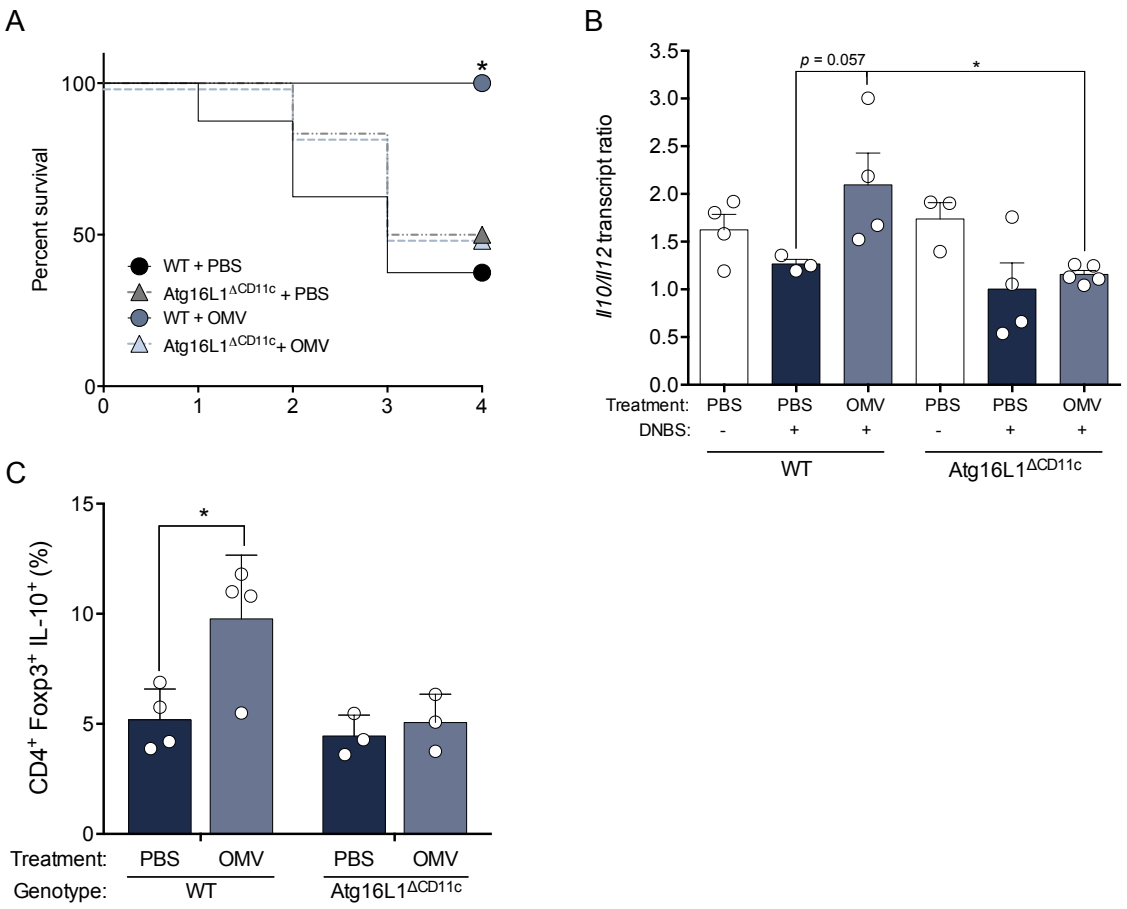

Fig. S8. *B. fragilis* OMV-mediated protection from colitis requires ATG16L1 in DCs.

(A) Survival cure of WT and Atg16L1$^{\Delta CD11c}$ mice orally treated with PBS or *B. fragilis* WT-OMV during DNBS colitis. Data are representative of at least 6 independent experiments, with 4 - 10 mice/group. * $p < 0.05$, Gehan-Breslow-Wilcoxon test. **(B)** MLNs isolated post-DNBS analyzed for *Il10*/*Il12* transcripts, as assessed by quantitative real-time RT-PCR. Transcripts were normalized to β-actin. **(C)** cLP lymphocytes isolated post-DNBS analyzed for IL-10 production among CD4^{+}Foxp3^{+} T$_{regs}$. Error bars represent S.E.M. * $p < 0.05$. Data are representative of at least 2 independent experiments, with 3-5 mice/group.

Fig. S9

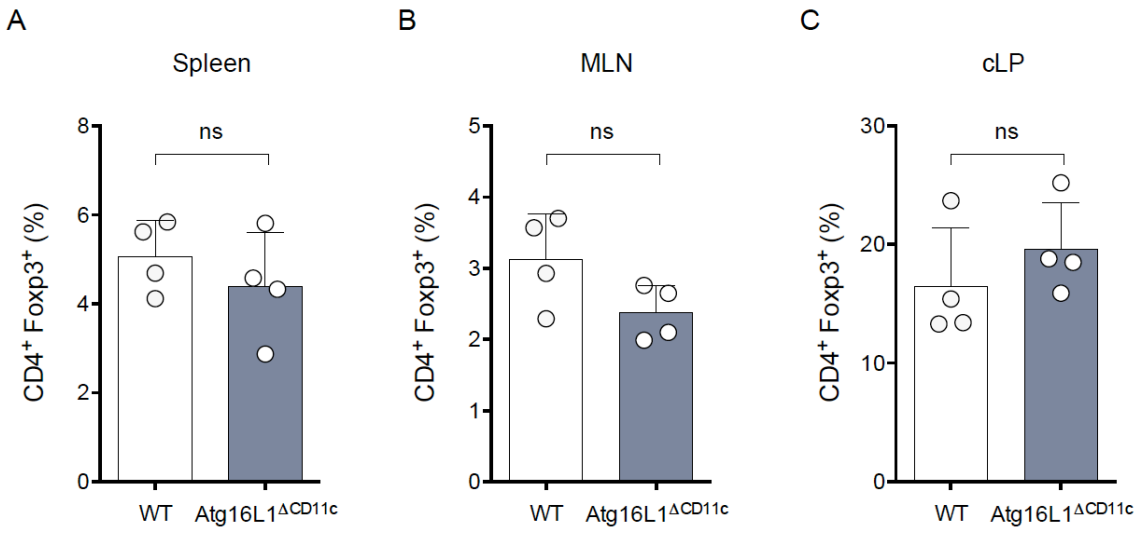

Fig. S9. *B. fragilis* OMV-mediated protection is not due to an overall defect in T_{reg} development in Atg16L1$^{\Delta CD11c}$ mice under naïve conditions.

Proportions of $CD4^+Foxp3^+$ T cells in **(A)** spleen, **(B)** MLNs and **(C)** cLP of WT and Atg16L1$^{\Delta CD11c}$ naïve mice. Error bars represent S.E.M. ns, not significant. Data are representative of at least 2 independent experiments, with 3-5 mice/group.

Fig. S10

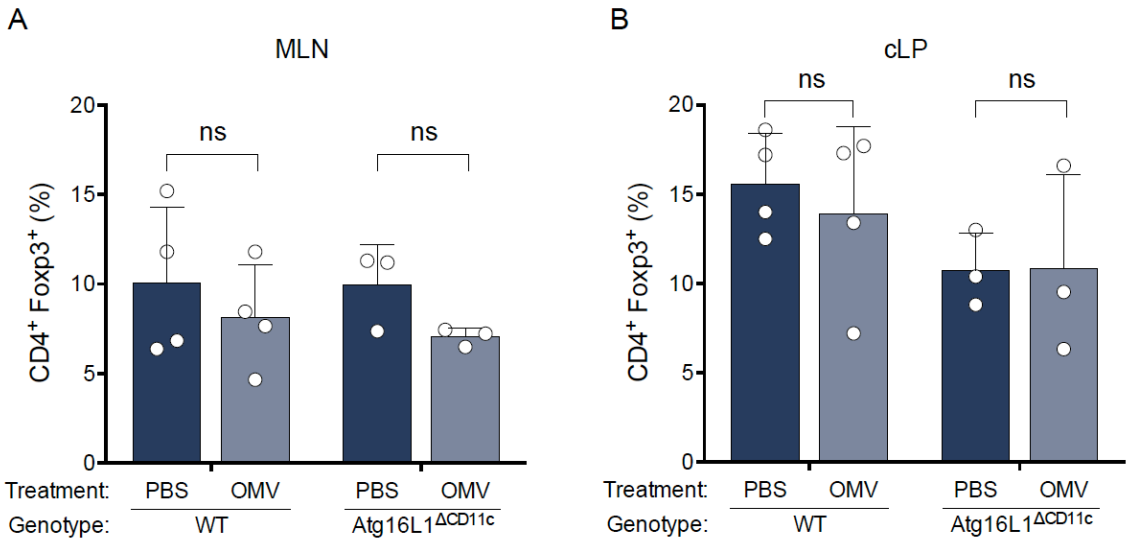

Fig. S10. *B. fragilis* OMV-mediated protection is not due to an overall defect in T_{reg} development in Atg16L1$^{\Delta CD11c}$ mice during colitis.

Proportions of CD4$^+$Foxp3$^+$ T cells in **(A)** MLNs and **(B)** cLP of WT and Atg16L1$^{\Delta CD11c}$ mice orally treated with PBS or *B. fragilis* WT-OMV during DNBS colitis. Error bars represent S.E.M. ns, not significant. Data are representative of at least 3 independent experiments, with 3-5 mice/group.

Fig. S11

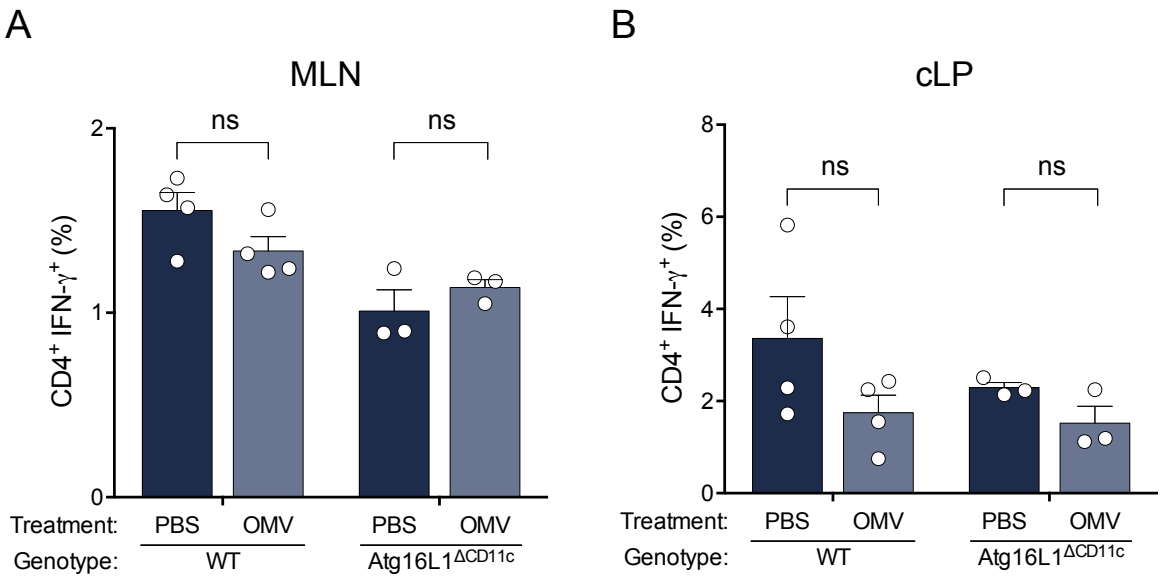

Fig. S11. CD4$^+$IFN-γ$^+$ populations are not significantly altered by *B. fragilis* WT-OMV treatment during DNBS colitis.

(A) MLN and **(B)** cLP lymphocytes isolated post-DNBS analyzed for IFN-γ production among CD4$^+$ T cells, as assessed by flow cytometry. Error bars represent S.E.M. ns, not significant. Data are representative of at least 2 independent experiments, with 3-4 mice/group.

Fig. S12

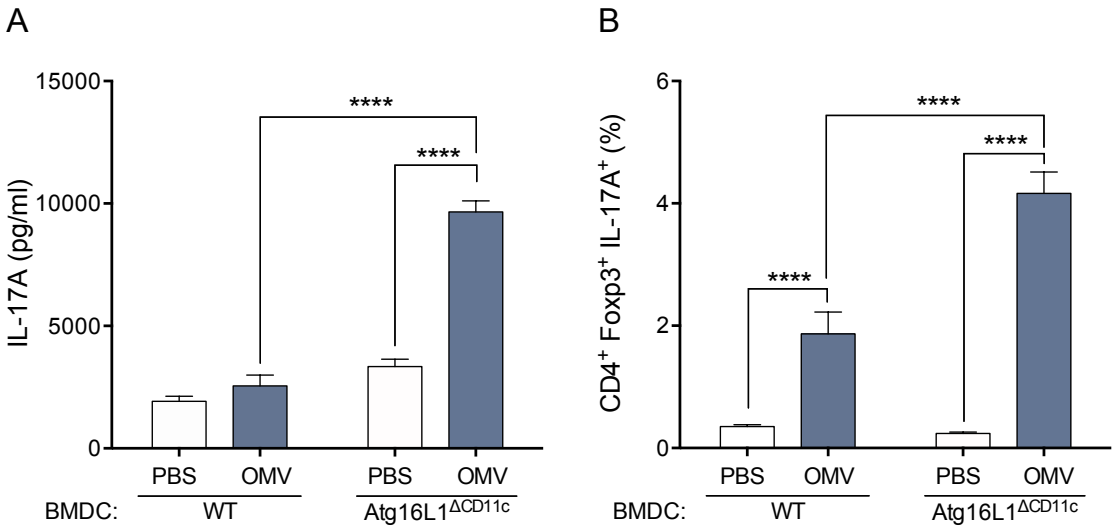

Fig. S12. OMV treatment of Atg16L1$^{\Delta CD11c}$ DCs promotes IL-17A production.

In vitro DC–T cell co-cultures with WT or Atg16L1$^{\Delta CD11c}$ DCs treated with PBS or *B. fragilis* WT-OMVs and analyzed for IL-17A by **(A)** ELISA and **(B)** ICCS among $CD4^+Foxp3^+$ T_{regs}. Error bars represent S.E.M. **** $p < 0.0001$. Data are representative of at least 3 independent experiments.

Fig. S13

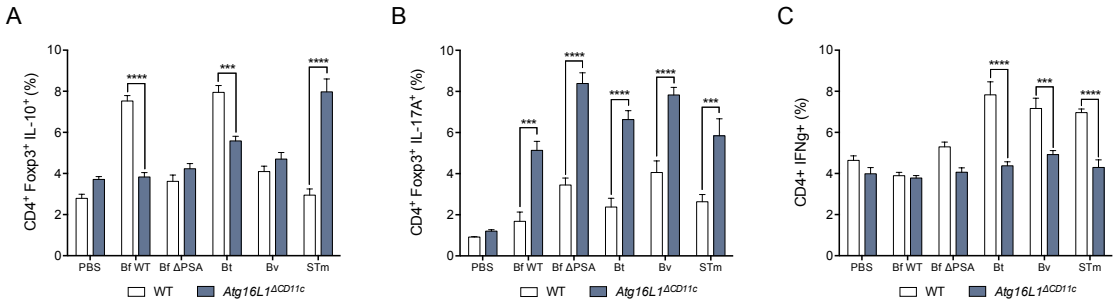

Fig. S13. Commensal and pathogen-derived OMVs differentially utilize ATG16L1 in CD11c$^+$ BMDCs.

Frequency of **(A)** CD4$^+$Foxp3$^+$IL-10$^+$ T_{regs}, **(B)** CD4$^+$Foxp3$^+$IL-17A$^+$ T cells and **(C)** CD4$^+$IFN-γ$^+$ T cells from DC–T cell co-cultures with WT or Atg16L1$^{\Delta CD11c}$ DCs treated with PBS, *B. fragilis* WT-OMV, ΔPSA-OMV, Bt-OMV, Bv-OMV, or *S.*Tm OMVs. Error bars represent S.E.M. *** $p < 0.001$, **** $p < 0.0001$. Data are representative of 3 independent experiments. Bt, *Bacteroides thetaiotamicron*; Bv, *Bacteroides vulgatus*; STm, *Salmonella enterica* serovar Typhimurium.

Fig. S14

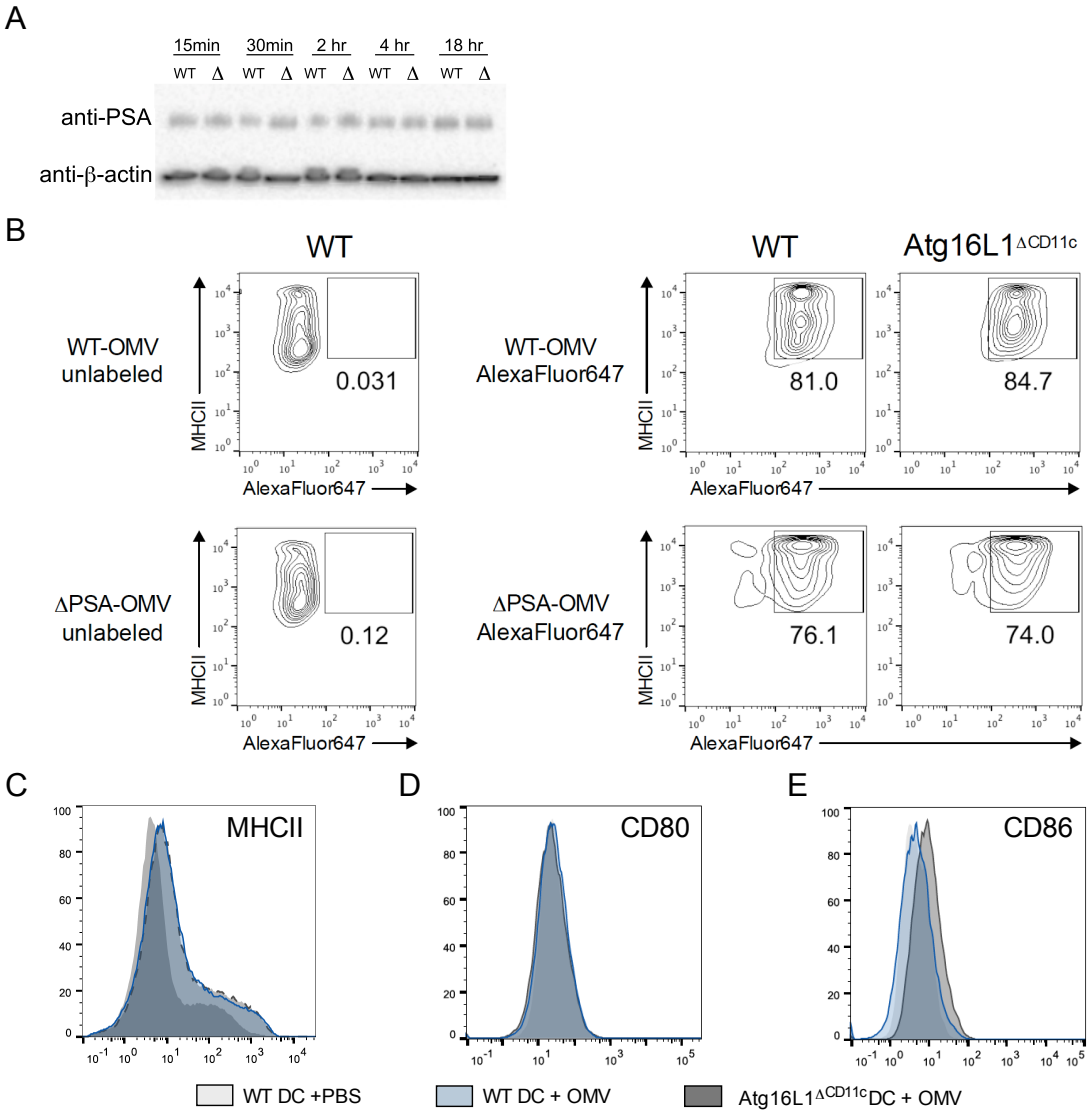

Fig. S14. Atg16L1$^{\Delta CD11c}$ DCs are not impaired in uptake of *B. fragilis*-labeled OMVs.

(A) WT and Atg16L1$^{\Delta CD11c}$ BMDCs were pulsed with WT-OMVs at indicated time points and analyzed for uptake of WT-OMVs. Treated DCs were analyzed by western blot and probed for PSA and β-actin. Δ, Atg16L1$^{\Delta CD11c}$ DCs. Data are representative of at least 4 independent experiments. **(B)** WT and Atg16L1$^{\Delta CD11c}$ BMDCs were pulsed with Click-iT-labeled-Alexa Fluor 647 WT- or ΔPSA-OMV for 3 h and analyzed for uptake of OMVs among live CD11c^{+}MHCII^{+} cells. Data are representative of at least 2 independent experiments. **(C** to **E)** Representative histograms of MHC II (C), CD80 (D) and CD86 (E) expression among live, CD11c^{+} cells upon PBS and WT-OMV treatment of WT or Atg16L1$^{\Delta CD11c}$ BMDCs. Data are representative of at least 4 independent experiments.

Fig. S15

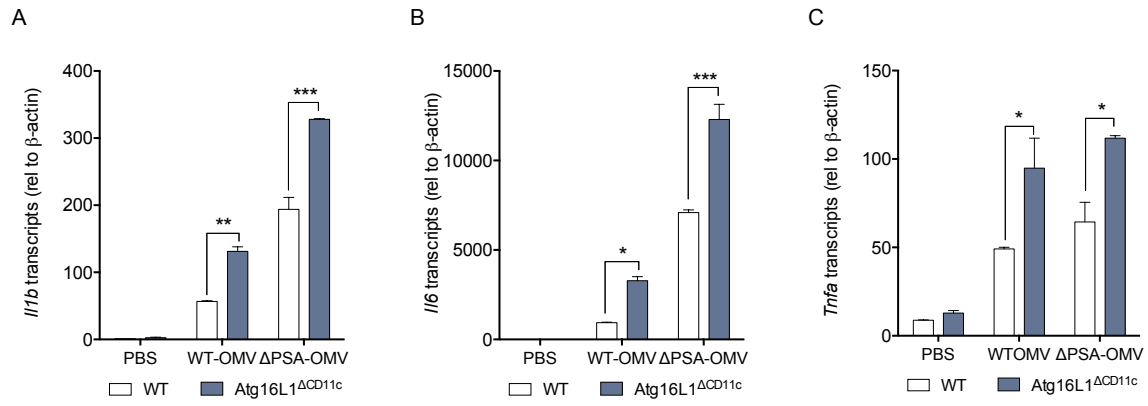

Fig. S15. Atg16L1$^{\Delta CD11c}$ DCs display a hyper-inflammatory cytokine profile.

Quantitative RT-PCR of **(A)** *Il1b*, **(B)** *Il6*, and **(C)** *Tnfa* in WT or Atg16L1$^{\Delta CD11c}$ BMDCs treated with PBS, WT-OMV or ΔPSA-OMV, relative to the β-actin. Error bars represent S.E.M. * $p < 0.05$, ** $p < 0.01$, and *** $p < 0.001$. Data are representative of at least 4 independent experiments.

Fig. S16

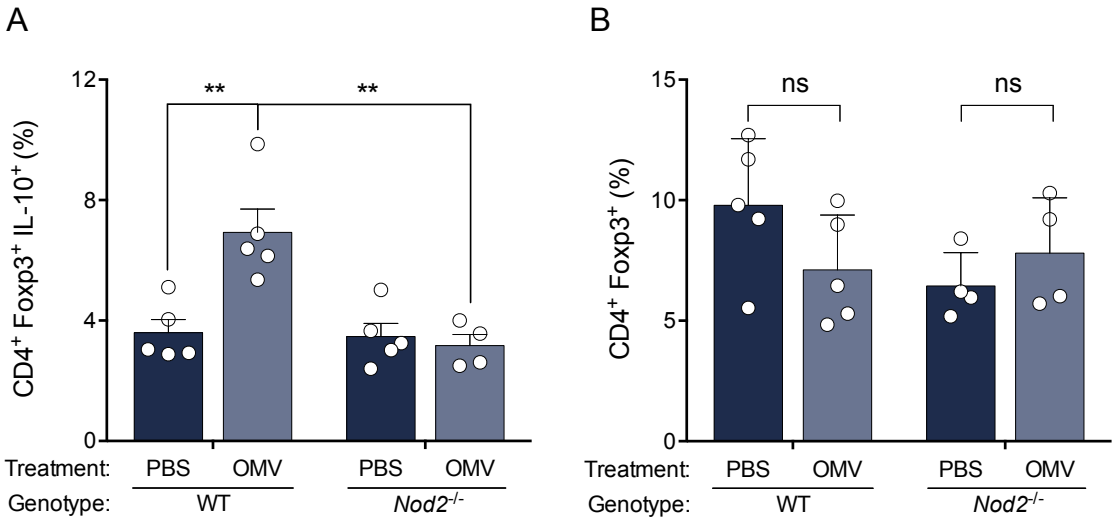

Fig. S16. Induction of CD4$^+$Foxp3$^+$IL-10$^+$ T$_{regs}$ in the colon during colitis is impaired in *Nod2*$^{-/-}$ mice.

(A) cLP lymphocytes isolated post-DNBS analyzed for IL-10 production among CD4$^+$Foxp3$^+$ T$_{regs}$. **(B)** Proportions of CD4$^+$Foxp3$^+$ T$_{regs}$ in MLNs of WT and *Nod2*$^{-/-}$ mice orally treated with PBS or *B. fragilis* WT-OMV during DNBS colitis. Error bars represent S.E.M. ** $p < 0.01$. ns, not significant. Data are representative of at least 2 independent experiments, with 4-5 mice/group.

Fig. S17

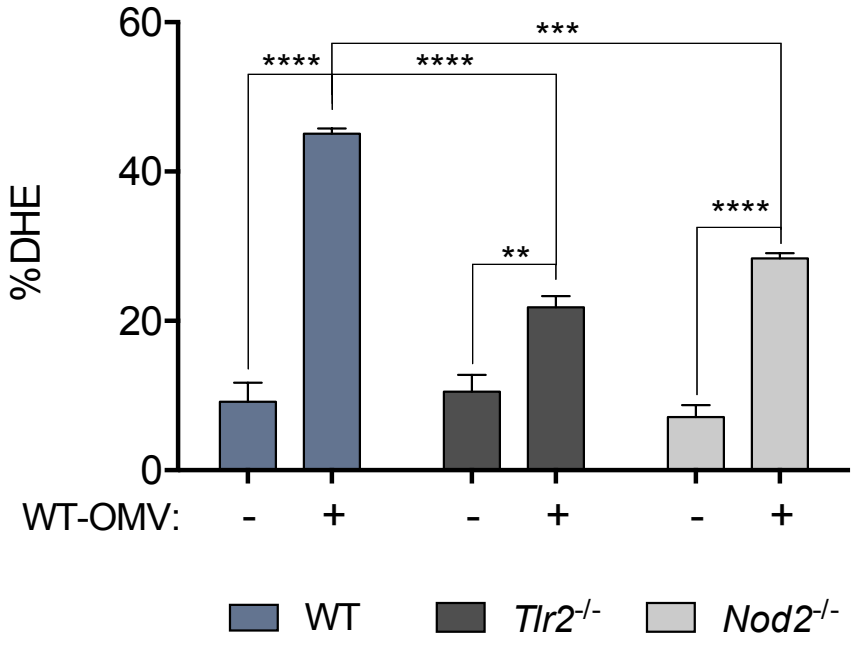

Fig. S17. TLR2 and NOD2 are involved in OMV-mediated induction of reactive nitrogen species (ROS), a feature of LAP.

WT, *Tlr2*$^{-/-}$, or *Nod2*$^{-/-}$ BMDCs were pulsed with WT-OMVs for 2h and ROS production was assessed by dihydroethidium (DHE), as measured for flow cytometry. Error bars represent S.E.M. ** $p < 0.01$, *** $p < 0.001$, **** $p < 0.0001$. Data are representative of 3 independent experiments.

Fig. S18

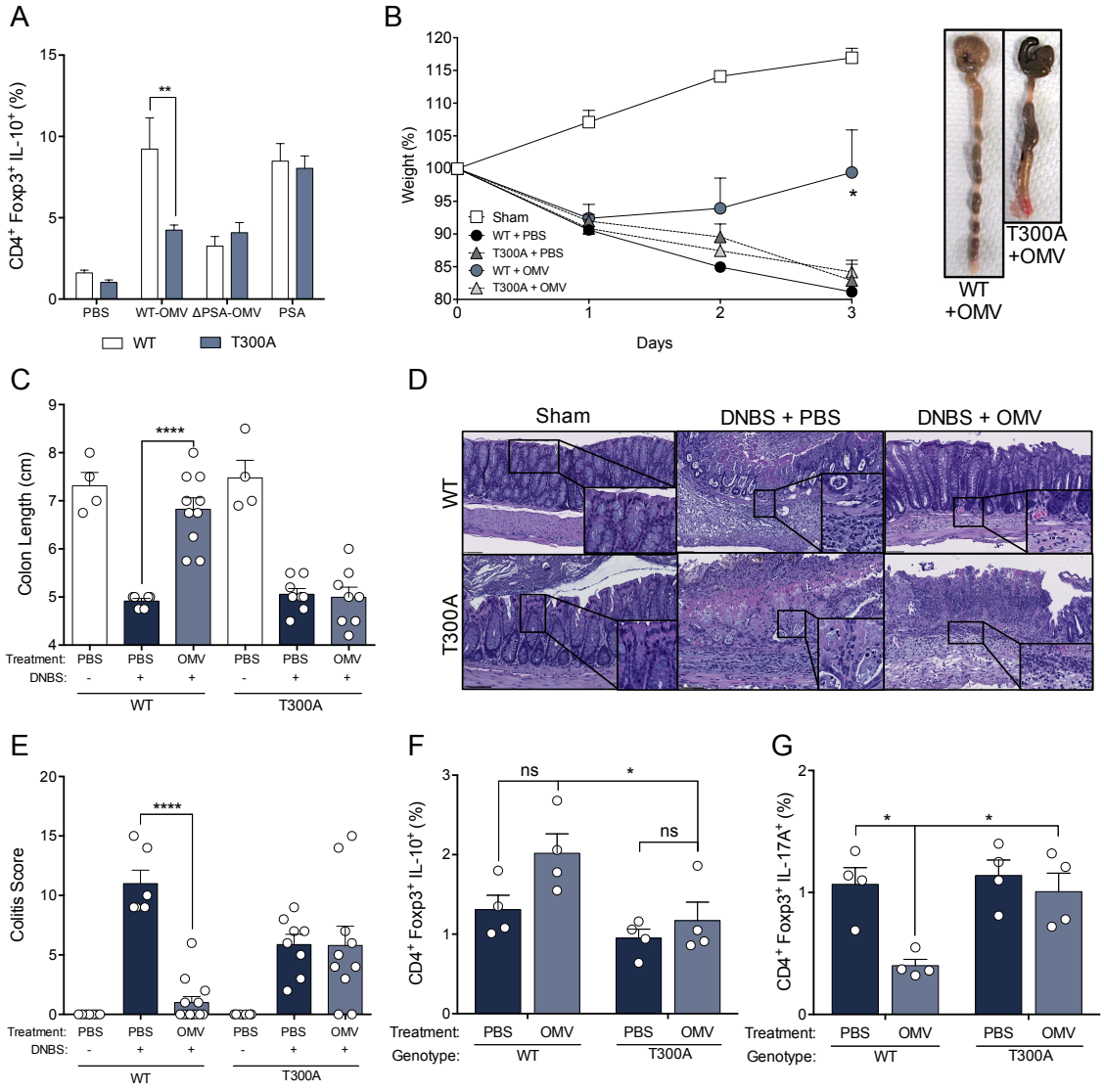

Fig. S18. ATG16L1 T300A transgenic mice are not protected from colitis by *B. fragilis* OMVs.

(A) Frequency of IL-10 among CD4$^+$Foxp3$^+$ T$_{regs}$ from DC–T cell co-cultures of WT and T300A BMDCs treated with PBS, *B. fragilis* WT-OMV, ΔPSA-OMV or purified PSA. **(B)** Weight loss and gross pathology, **(C)** colon length, **(D)** H & E sections, **(E)** and colitis scores of WT and T300A mice orally treated with PBS or *B. fragilis* WT-OMV during DNBS colitis. MLN lymphocytes isolated post-DNBS analyzed for **(F)** IL-10 and **(G)** IL-17A production among CD4$^+$Foxp3$^+$ T$_{regs}$, as assessed by flow cytometry. Error bars represent S.E.M. * $p < 0.05$, ** $p < 0.01$, **** $p < 0.0001$. Data are representative of at least 3 independent experiments, with 3 – 5 mice/group.

Table S1

Sample ID	Disease Status	Genotype	Sex	Age	Medications
CTL01	Normal	T300 (AA)	F	32	N/A
CTL02	Normal	T300 (AA)	F	40	N/A
CTL03	Normal	T300 (AA)	F	63	N/A
CD04	CD	T300 (AA)	M	57	N/A
CD05	CD	T300 (AA)	M	53	N/A
CD06	CD	T300 (AA)	M	39	N/A
CTL07	Normal	T300A (GG)	F	44	N/A
CTL08	Normal	T300A (GG)	F	68	N/A
CD09	CD	T300A (GG)	F	28	mercaptopurine (Purinethol); mesalamine (Apriso)
CD10	CD	T300A (GG)	F	27	adalimumab (Humira); *Bifidobacterium infantis* (Align); multivitamin; Noreth A-ET Estra/FE Fumarate(Lo Loestrin FE PO), Omega-3 Fatty Acids-Vitamin E (fish Oil); Resveratrol
CD11	CD	T300A (GG)	M	37	N/A
CD12	CD	T300A (GG)	M	23	N/A

Table S1. Human subjects.

Sample ID, disease status, *ATG16L1* genotype, sex, age, and medications taken at time of blood collection. CTL, control; CD, Crohn's disease; F, female; M, male.

References

41. S. Hwang, N. S. Maloney, M. W. Bruinsma, G. Goel, E. Duan, L. Zhang *et al.*, Nondegradative role of Atg5-Atg12/ Atg16L1 autophagy protein complex in antiviral activity of interferon gamma. *Cell Host Microbe* **11**, 397-409 (2012); published online EpubApr 19 (S1931-3128(12)00094-7 [pii]10.1016/j.chom.2012.03.002).

42. K. Matsunaga, T. Saitoh, K. Tabata, H. Omori, T. Satoh, N. Kurotori *et al.*, Two Beclin 1-binding proteins, Atg14L and Rubicon, reciprocally regulate autophagy at different stages. *Nature cell biology* **11**, 385-396 (2009); published online EpubApr (10.1038/ncb1846).

43. M. Kundu, T. Lindsten, C. Y. Yang, J. Wu, F. Zhao, J. Zhang *et al.*, Ulk1 plays a critical role in the autophagic clearance of mitochondria and ribosomes during reticulocyte maturation. *Blood* **112**, 1493-1502 (2008); published online EpubAug 15 (10.1182/blood-2008-02-137398).

44. M. J. Coyne, A. O. Tzianabos, B. C. Mallory, V. J. Carey, D. L. Kasper, L. E. Comstock, Polysaccharide biosynthesis locus required for virulence of Bacteroides fragilis. *Infection and immunity* **69**, 4342-4350 (2001); published online EpubJul (10.1128/IAI.69.7.4342-4350.2001).

45. S. Patrick, J. H. Reid, Separation of capsulate and non-capsulate Bacteroides fragilis on a discontinuous density gradient. *Journal of medical microbiology* **16**, 239-241 (1983); published online EpubMay.

46. C. C. Kurtz, I. Drygiannakis, M. Naganuma, S. Feldman, V. Bekiaris, J. Linden *et al.*, Extracellular adenosine regulates colitis through effects on lymphoid and nonlymphoid cells. *American journal of physiology. Gastrointestinal and liver physiology* **307**, G338-346 (2014); published online EpubAug 1 (10.1152/ajpgi.00404.2013).